Advances in Aircraft and Spacecraft Science, *Vol. 1, No. 1 (2014) 093-123*
DOI: http://dx.doi.org/10.12989/aas.2014.1.1.093

A variational asymptotic approach for thermoelastic analysis of composite beams

Qi Wang*[1] and Wenbin Yu[2]

[1]*Department of Mechanical and Aerospace Engineering, Utah State University, Logan, Utah 84322-4130, USA*
[2]*School of Aeronautics and Astronautics, Purdue University, West Lafayette, IN, USA*

(Received August 28, 2013, Revised September 25, 2013, Accepted September 28, 2013)

Abstract. A variational asymptotic composite beam model has been developed for thermoelastic analysis. Composite beams, including sandwich structure and laminates, under different boundary conditions are examined. Previously developed beam model, which is based on variational-asymptotic method, is extended to incorporate temperature-dependent materials experiencing large temperature changes. The recovery relations have been derived so that the temperatures, heat fluxes, stresses, and strains can be recovered over the cross-section. The present theory is implemented into the computer program VABS (Variational Asymptotic Beam Sectional analysis). Numerical results are compared with the 3D analysis for the purpose of demonstrating advantages of the present theory and use of VABS.

Keywords: variational asymptotic method; composite beam; finite element method; thermoelasticity; VABS; finite temperature change

1. Introduction

Beam structure, or sometimes called slender structure, is defined as a structure having one of its dimensions much greater than the other two. Many engineering components can be idealized as beams. Typical applications of beam structures in civil engineering are bridges: an arch bridge is composed of both curved and prismatic beams; a truss bridge is mainly supported by trusses, which can be viewed as assembly of beams or beam girders. A large number of building and machine parts are beam-like structures: joists, lever arms, shafts, and turbine blades, etc. Examples of beam-like structures in aeronautics include helicopter rotor blades and high aspect-ratio wings.

Thermoelastic analysis is meant to describe the thermal and mechanical behaviors of the engineering structures subject to combined loads. Based on the quasisteady theory of linear thermoelasticity, the thermal problem separates into two problems to be solved consecutively: the heat conduction problem and the one-way coupled thermoelastic problem. Due to their special characteristics like high-strength and light-weighted, the composite beam structure often works under extreme conditions in aerospace systems. For example, the thermal protection system of space vehicles has to withstand temperatures ranging from 300°C to 1500°C during ascent and

*Corresponding author, Curently, researcher Engineer at National Renewable Energy Laboratoy, E-mail: Qi.Wang@aggiemail.usu.edu
[a] Associate Professor, E-mail: wenbinyu@purdue.edu

http://www.techno-press.org/?journal=aas&subpage=7 ISSN: 2287-528X (Print), 2287-5271 (Online)

reentry, while in the outer space, the vehicle surface may be subjected to temperatures up to - 150°C (Bapanapalli *et al.* 2006). Moreover, composite materials are more sensitive and vulnerable to temperature change than their isotropic counterparts. For composites, the thermal expansion coefficients of different constituents of the material are usually dramatically different from each other resulting in high stresses due to temperature changes from the stress free environment. The traditional constitutive framework of thermoelasticity which is based on temperature-independent condition, small temperature assumption, and small strain assumption may not work for structures experiencing large temperature changes. For most cases, it is still reasonable to assume the strains are small. However, the temperature change cannot be considered as "small". And also, if the temperature changes are large enough, the material properties including elastic constants, coefficients of thermal expansion become temperature dependent (Okamoto *et al*. 2003, Noda 1991).

Theories of composite beam structure, including classical laminate theory (Bickford 1982) and refined laminate theory (Kant and Manjunath 1989, Soldatos and Elishakoff 1992, Marur and Kant 1997, Heyliger and Reddy 1988), have been reviewed in detail in the textbook by Reddy (2003). Some of these theories, both classical and refined theories, have been extended to deal with the thermal problem of composite beams (Tanigawa *et al*. 1989, Khdeir and Reddy 1999). Copper and Pilkey (2002) developed an analytical thermoelastic solution for beams with arbitrary temperature distribution. The problem is considered as a plane strain problem and the maximum stresses on a certain cross-section are validated with 3D solution and strength of materials solution. Huang *et al*. (2007) investigated a functionally graded anisotropic cantilever beam subject to thermal and mechanical loads. The problem is solved analytically based on the plane stress assumption. Rao and Sinha (1997) proposed a finite element model to deal with the coupled thermoelastic analysis of composite beams. This model is based on Timoshenko beam theory and plane stress assumption, and the temperature is also assumed to be uniform through the thickness of the beam. It cannot yield the thermal and mechanical field over the cross-section but only an averaged temperature and the stress resultants. Vidal and Polit (2006) developed a three-noded thermoelastic beam element for composite beam analysis. The thermal problem separates into two problems to be solved consecutively: the heat conduction problem to solve for the thermal field and the one-way coupled thermoelastic problem for the structure under a prescribed thermal field. This work allowed the variations of thermal and mechanical fields along the thickness of cross-section. Trigonometric functions are used in the assumed displacement field to avoid shear correction factors. But one dimension over the cross-section, say the width, is neglected in the solution. Kapuria *et al*. (2003) reported a beam model based on zigzag theory for thermal analysis. By modifying the third-order zigzag model, the contribution of thermal expansion coefficient along thickness of the beam is considered while this model still neglects the variations along width on the cross-section. Another notable work was that of Ghiringhelli (1997a, b), where the thermal problem of general composite beams is solved using a finite element semi-discretization approach. The thermal field within a beam cross-section subject to prescribed boundary conditions was attained first taking into account any kind of thermal anisotropy or inhomogeneity. Then the thermoelastic problem in a beam having arbitrary nonhomogeneous, anisotropic material properties over the cross-section was solved under the thermal loads obtained in the previous step. This model can capture the thermal and mechanical fields on the cross-sections.

Most of the previous described beam models can be classified into *ad hoc* models, which are based on *a priori* kinematic assumptions, and asymptotic models, which are derived by asymptotic expansions of the displacement field. The advantage of *ad hoc* models is that the reduced

governing equations can be derived in a straightforward manner using variational statements; and this procedure is simple and straight forward for engineers to understand. While the disadvantages are: (1) it is a common source of error that the kinematic assumptions contradict each other in 1D and 2D analysis, (2) it is difficult to determine the shear correction factors needed in refined theories for composite laminated structures, and (3) it is difficult to make assumptions on distributions of mechanical and thermal fields over the cross sections for composite materials. Comparing with *ad hoc* models, the asymptotic method could develop elegant and rigorous models; however, it is very cumbersome and restricted from both geometric and material points of view.

Variational-asymptotic method (VAM) is a powerful mathematical approach which is first proposed by Berdichevsky (1979) about three decades ago. It is applicable to any problem that can be posed in terms of seeking the stationary points of a functional involving some inherent small parameters. This method combines both merits of variational methods and asymptotic methods thus it does not rely on any *ad hoc* assumptions while is systematic and easy to be implemented numerically. Hodges *et al*. (1992) first applied VAM to yield the cross-sectional properties for prismatic beam. Cesnik and Hodges (1993) extended the model taking into consideration the influence of initial curvatures. Researchers have proposed the refined theories based on VAM (Popescu and Hodges 2000, Yu *et al*. 2002). Yu *et al*. (2012) reported the recent updates on this theory. Recently, the authors have extended VAM for thermal problem of composite beams (Wang and Yu 2011, 2013). Based on the previous work, the current paper presents a model for thermoelastic analysis of composite beams under different loadings and boundary conditions and features a new framework of thermoelasticity.

2. Beam kinematics

As sketched in Fig. 1(a), a beam can be represented by a reference line r, described by its arc-length x_1, and a typical reference cross-section normal to the reference line, described by local Cartesian coordinates x_α. (Here and throughout the paper, Greek indices assume values 2 and 3 while Latin indices assume 1, 2, and 3. Repeated indices are summed over their range except where explicitly indicated.) At each point along the reference line, an orthonormal triad $\mathbf{b}_i$ is introduced such that $\mathbf{b}_i$ is tangent to x_i. Any point of the undeformed beam structure is then located by the position vector $\hat{\mathbf{r}}$ as

$$\hat{\mathbf{r}}(x_1, x_2, x_3) = \mathbf{r}(x_1) + x_\alpha \mathbf{b}_\alpha \tag{1}$$

where $\mathbf{r}$ is the position vector of a point on the reference line, $\mathbf{r}' = \mathbf{b}_1$ and $(\,)'$ means the partial derivative with respect to x_1. It is noted that $\mathbf{b}_i$ could be functions of x_1 due to existence of initial curvatures or twist.

When the beam deforms, the triad $\mathbf{b}_i$ rotates to coincide with a new triad $\mathbf{B}_i$. Here $\mathbf{B}_1$ is not tangent to the deformed beam reference line if the transverse shear deformation is considered. $\mathbf{B}_i$ coincides with $\mathbf{b}_i$ before deformation and during deformation they can be related as

$$\mathbf{B}_i = \mathbf{C}^{Bb}\mathbf{b}_i = C_{ij}^{Bb}\mathbf{b}_j \tag{2}$$

where $\mathbf{C}^{Bb} = C_{ij}^{Bb}\mathbf{b}_j\mathbf{b}_i$ denotes the rotation tensor, and C_{ij}^{Bb} are the components of the corresponding direction cosine matrix. The deformed position vector, **R**, of the point which had $\hat{\mathbf{r}}$

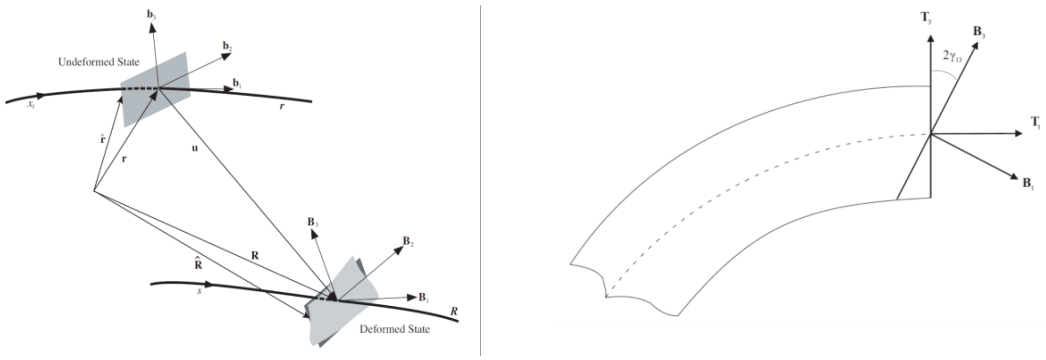

(a) Schematic of beam deformation (b) Transverse shear deformation

Fig. 1 Beam kinematics: (a) Schematic of beam deformation: undeformed and deformed states and (b) Coordinate systems used for transverse shear formulation

in the undeformed state can be express as

$$\mathbf{R}(x_1,x_2,x_3)=\mathbf{r}(x_1)+\mathbf{u}(x_1)+x_\alpha\mathbf{B}_\alpha+\overline{w}_i(x_1,x_2,x_3)\mathbf{B}_i \tag{3}$$

where $\mathbf{u}=u_i\mathrm{b}_i$ is the displacement vector of the reference line from the reference configuration and $\overline{w}_i(x_1,x_2,x_3)$ are the warping functions.

Although the expression in Eq. (3) is mathematically correct, it is not convenient for carrying out the dimensional reduction from the original 3D model to a 1D beam model using the variational-asymptotic method. Instead, we introduce another triad $\mathbf{T}_i$ associated with the deformed beam (see Fig. 1(b)), with $\mathbf{T}_1$ tangent to the deformed beam reference line and $\mathbf{T}_\alpha$ determined by a rotation about $\mathbf{T}_1$. The difference in the orientations of $\mathbf{T}_i$ and $\mathbf{B}_i$ is due to small rotations associated with transverse shear deformation. The relationship between these two basis vectors can be expressed as

$$\begin{Bmatrix}\mathbf{B}_1\\ \mathbf{B}_2\\ \mathbf{B}_3\end{Bmatrix}=\begin{bmatrix}1 & -2\gamma_{12} & -2\gamma_{13}\\ 2\gamma_{12} & 1 & 0\\ 2\gamma_{13} & 0 & 1\end{bmatrix}\begin{Bmatrix}\mathbf{T}_1\\ \mathbf{T}_2\\ \mathbf{T}_3\end{Bmatrix} \tag{4}$$

where $2\gamma_{12}$ and $2\gamma_{13}$ are the small angles characterizing the transverse shear deformation, and we know $2\gamma_{1\alpha}<<1$ due to the small strain assumption. The distinction between these two frames is important for the development of different levels of approximation.

The material point having position vector $\hat{\mathbf{r}}$ in the undeformed beam can also be expressed as

$$\mathbf{R}(x_1,x_2,x_3)=\mathbf{r}(x_1)+\mathbf{u}(x_1)+x_\alpha\mathbf{T}_\alpha(x_1)+w_i(x_1,x_2,x_3)\mathbf{T}_i(x_1) \tag{5}$$

where w_i are the components of warping resolved in $\mathbf{T}_i$ base system. Note that in this formulation we choose $\mathbf{T}_1$ to be tangent to the deformed beam reference line, which means that we classify the transverse shear deformation as part of the warping field. Within the framework of small strains this neither introduces any additional approximations nor results in any loss of

information. Eq. (5) is four times redundant because of the way warping was introduced. For simplicity of analysis we are choosing here a centroidal cross-sectional coordinate system, which can easily be relaxed if necessary. To remove the redundancy of the warping field, the following four constraints can be used

$$\langle w_i \rangle = 0 \quad \langle w_{2,3} - w_{3,2} \rangle = 0 \tag{6}$$

where angle bracket $\langle \quad \rangle$ denotes integration over the cross-section. The constraints in Eq. (6) can be written in matrix form as

$$\langle \Gamma_c w \rangle = 0 \tag{7}$$

with $w = \lfloor w_1 \; w_2 \; w_3 \rfloor^T$ and

$$\Gamma_c = \begin{bmatrix} 1 & 0 & 0 \\ 0 & 1 & 0 \\ 0 & 0 & 1 \\ 0 & \partial_3 & \partial_2 \end{bmatrix} \tag{8}$$

where $\partial_\alpha = \dfrac{\partial}{\partial x_\alpha}$.

3. Heat conduction analysis

3.1 3D formulation

The 3D steady heat conduction problem of a composite beam is governed by the variation of the following functional

$$\Pi = U_T - I_T \tag{9}$$

where we term U_T as the thermal potential and I_T as the power input with expressions as

$$U_T = \int_0^l \left\langle \left\langle \frac{1}{2} (\nabla T)^T K \nabla T \right\rangle \right\rangle dx_1 \equiv \int_0^l \mathrm{U}_T \, dx_1 \tag{10}$$

and

$$I_T = \int_0^l \left[<< QT >> + \oint \bar{q} T \sqrt{c} \, ds \right] dx_1 + \langle \bar{q}_e T \rangle \Big|_{x_1 = L} + \langle \bar{q}_e T \rangle \Big|_{x_1 = 0} \tag{11}$$

T is the 3D temperature field, K is the conductivity matrix representing the second-order conductivity tensor expressed in the triad $\mathbf{b}_i$, Q is the density of internal heat source, $\bar{q}$ is the given heat flux on the lateral boundary surfaces $\partial\Omega$, and $\bar{q}_e$ is the given heat flux on the end surfaces. The notation $\langle\langle \cdot \rangle\rangle = \int_s \cdot \sqrt{g} \mathrm{d}x_2 \mathrm{d}x_3$, g is the determinant of the metric tensor for the

undeformed geometry $g_{ij} = \det(g_i \cdot g_j)$ with $\sqrt{g} = 1 - x_2 k_3 + x_3 k_2$. $c = g + \left(x_2 \frac{dx_2}{ds} + x_3 \frac{dx_3}{ds} \right)^2$ with ds as the differential arc length along the boundary curve. k_1 is the initial twist and k_α are the initial curvatures. It is pointed out that if the convection heat transfer is taken into consideration, one more term should be included in the power input I_T as $\int_0^l \oint -\frac{1}{2} h_c T (T - 2T_\infty) \sqrt{c} ds dx_1$ where h_c is the convective heat transfer coefficient and T_∞ is the temperature of adjacent fluid outside the boundary layer. The temperature gradient ∇T in a curvilinear coordinate system can be expressed as

$$\nabla T = \frac{\partial T}{\partial x_i} \mathbf{g}^i \tag{12}$$

with the base vectors defined as

$$\mathbf{g}_i = \frac{\partial \hat{\mathbf{r}}}{\partial x_i} \qquad \mathbf{g}^i = \frac{e_{ijk} \mathbf{g}_j \times \mathbf{g}_k}{2\sqrt{g}} \tag{13}$$

where e_{ijk} are the components of the permutation tensor in a Cartesian coordinate system.

There are two types of thermal load for heat conduction analysis.

• Thermal load case 1: temperature field is not prescribed at any point over the cross-section except the end surfaces at $x_1 = 0$ and $x_1 = l$ (see Fig. 2(a)). For this case we are free to use the following change of variables for the 3D temperature field

$$T(x_1, x_2, x_3) = \mathbb{T}(x_1) + w_T(x_1, x_2, x_3) \tag{14}$$

with the 1D temperature variable $\mathbb{T}(x_1)$ defined as the average of T over the cross-section and w_T is the thermal warping functions that describe the difference between the 3D temperature field and its cross-sectional average. According to the definition, we have the following constraint on thermal warping functions

$$\langle w_T(x_1, x_2, x_3) \rangle = 0 \tag{15}$$

and this should be valid for all the surfaces along the beam span including the end surfaces.

• Thermal load case 2: temperature is prescribed at least one point of the cross-section along the beam span (see Fig. 2(b)). For this case, we lose the freedom of introducing the 1D temperature variable $\mathbb{T}(x_1)$ as what we did in Eq. (14), and all the 3D temperature field must be represented by the thermal warping function as

$$T(x_1, x_2, x_3) = w_T(x_1, x_2, x_3) \tag{16}$$

And we cannot constrain the thermal warping functions as we did in Eq. (13) either.

3.2 Dimensional reductional of case 1

In view of Eq. (14), the temperature gradient components in Eq. (12) can be expressed in the following column matrix

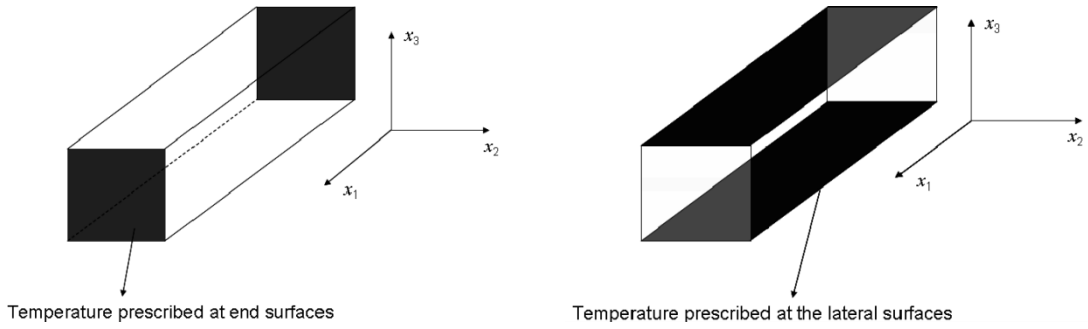

(a) Thermal load case 1 (b) Thermal load case 2

Fig. 2 Two types of heat conduction problem: (a) Thermal load case 1: temperature prescribed at the end surfaces of the beam and (b)Thermal load case 2: temperature prescribed at the lateral surfaces of the beam

$$\nabla T = e_1 \mathrm{T}' + \Gamma_T w_T + \Gamma_{RT} w_T + e_1 w_T' \tag{17}$$

with $e_1 = \frac{1}{\sqrt{g}} \lfloor 1 \quad 0 \quad 0 \rfloor^T$, T' as 1D temperature gradient, and

$$\Gamma_T = \begin{bmatrix} 0 \\ \partial_2 \\ \partial_3 \end{bmatrix} \quad \Gamma_{RT} = \frac{1}{\sqrt{g}} \begin{bmatrix} k_1(x_3\partial_2 - x_2\partial_3) \\ 0 \\ 0 \end{bmatrix} \tag{18}$$

3.2.1 Zeroth-order approximation

Substituting Eq. (17) into Eq. (9), we can obtain the first approximation of the functional as

$$\prod_0 = \int_0^l \left[U_{T0} - \left(\langle Q \rangle + \oint_{\partial\Omega} \bar{q} ds \right) T \right] dx_1 - \left\langle \bar{q}_e T \right\rangle \Big|_{x_1 = l} - \left\langle \bar{q}_e T \right\rangle \Big|_{x_1 = 0} \tag{19}$$

where

$$\mathrm{U}_{T0} = \left\langle \frac{1}{2} \left(e_1 \mathrm{T}' + \Gamma_T w_T \right)^T K \left(e_1 \mathrm{T}' + \Gamma_T w_T \right) \right\rangle \tag{20}$$

Here terms higher than $O(\nu \mathrm{T}'^2)$ are neglected, and ν denotes the order of heat conduction coefficients. It is clear that the thermal warping functions can be solved by minimizing the zeroth-order thermal potential U_{T0} subject to the constraint in Eq. (15) as other terms do not contain $w_T(x_1, x_2, x_3)$.

To deal with the arbitrary cross-sectional geometry and anisotropic materials, we turn to the finite element method to find the stationary value of the functional. The thermal warping field can be discretized as

$$w_T(x_1, x_2, x_3) = S(x_2, x_3)V_T(x_1) \tag{21}$$

with $S(x_2, x_3)$ representing the matrix of finite element shape functions, and V_T as a column matrix of the nodal values of the thermal warping over the cross-section.

Substituting Eq. (21) back into Eq. (20) one obtains

$$2U_{T0} = V_T^T E_T V_T + 2V_T^T D_T T' + \bar{K} T'^2 \tag{22}$$

where the newly introduced matrices are defined as

$$\begin{aligned} E_T &= \left\langle \left[\Gamma_T S\right]^T K \left[\Gamma_T S\right] \right\rangle \\ D_T &= \left\langle \left[\Gamma_T S\right]^T K e_1 \right\rangle \\ \bar{K} &= \left\langle K_{11} \right\rangle \end{aligned} \tag{23}$$

Minimizing Eq. (22) subject to constraints in Eq. (15), we can obtain the thermal warping function in the following form

$$V_T = \bar{V}_{T0} T' = V_{T0} \tag{24}$$

Having solved $\bar{V}_T$, we can approximate the original functional in Eq. (19) using the following 1D functional

$$\prod_0 = \int_0^l \left[U_{T0} - \left(\langle Q \rangle + \oint_{\partial\Omega} \bar{q} ds \right) T \right] dx_1 - \left\langle \bar{q}_e T \right\rangle \Big|_{x_1=l} - \left\langle \bar{q}_e T \right\rangle \Big|_{x_1=0} \tag{25}$$

and

$$U_{T0} = \frac{1}{2}\left(\bar{V}_{T0}^T D_T + \bar{K}\right) T'^2 \equiv \frac{1}{2} \bar{K}_0 T'^2 \tag{26}$$

The scalar $\bar{K}_0$ can be viewed as a generalized heat conduction coefficient of a classical model for composite beams. Now we have constructed a reduced beam model under thermal load case 1 for heat conduction analysis. It is clear that the 1D constitutive model in Eq. (26) is asymptotically correct through the order of $O(\nu T'^2)$.

3.2.2 Discussion on convection heat transfer

It is known that there are three modes of heat transfer: conduction, convection, and radiation. In this chapter, a conduction model for beam analysis is constructed. Now this model is extended to incorporate convection heat transfer for thermal load case 1. An important application of convection is the analysis of a cooling fin.

The convection heat transfer is governed by Newton's law of cooling (Reddy 2008), which states that at a solid-fluid interface the heat flux is related to the difference between the temperature at the interface and that in the fluid

$$q_n = h_c(T - T_\infty) \tag{27}$$

where h_c is the heat transfer coefficient or film conductance. The functional that governs convection can be written as

$$\Pi_h = \int_0^l \left(\mathrm{U}_T - \mathrm{I}_{Th} \right) dx_1 \tag{28}$$

where $I_{Th} = -\oint (\frac{1}{2} h_c T^2 - h_c T T_\infty) \sqrt{c} ds$. Substitute Eq. (17) and Eq. (14) into Eq. (28), the first approximation can be written as

$$\prod_{h0} = \int_0^l \left[U_{T0} + \oint \frac{1}{2} h_c (T^2 - 2T\mathrm{T}_\infty) \sqrt{c} ds \right] dx_1 \tag{29}$$

Here terms are kept up to the order of $O(\nu \mathrm{T}'^2)$. From this equation we can see that the convection does not influence the zeroth-order solution of warping function. Thus, the governing functional for the first approximation can be written as

$$\prod_{h0} = \int_0^l \left[\frac{1}{2} \overline{K}_0 \mathrm{T}'^2 + \oint \frac{1}{2} h_c (\mathrm{T}^2 - 2\mathrm{T} T_\infty) \sqrt{c} ds \right] dx_1 \tag{30}$$

where $\overline{K}_0$ was found in Eq. (26). Carrying out calculus of variations to the above 1D functional, we obtain the following governing equation

$$\overline{K}_0 T'' + \oint h_c (\mathrm{T} - T_\infty) \sqrt{c} ds = 0 \tag{31}$$

with boundary conditions

$$\mathrm{T}(0) = T_0 \tag{32}$$

$$\mathrm{T}'(l) = 0 \tag{33}$$

where T_0 is the temperature at the end of beam. The 1D temperature T can be obtained by solving this boundary value problem.

3.2.3 First-order approximation

To obtain the first-order approximation with respect to initial twist and curvatures, we simply perturb the thermal warping function as

$$V_T = V_{T0} + V_{TR} \tag{34}$$

where $V_{TR} \sim O(\breve{h} \mathrm{T}')$ and $\breve{h}$ denotes the order of h/R and h/l, *i.e.*, $\breve{h} \sim h/R \sim h/l$ with h, l, and R the characteristic dimensions of the cross-section, wavelength of deformation, and radius of initial curvatures and twist, respectively.

Now we proceed to solve for the first-order approximation of the thermal warping function, V_{TR}. Substituting Eq. (34) along with Eq. (24) into Eq. (10), and neglecting all the terms higher than $O(\nu \mathrm{T}'^2 \breve{h}^2)$, we obtain

$$
\begin{aligned}
2U_{T1} &= 2U_{T0} + 2V_{T0}^T D_{Re}\mathrm{T}' + V_{T0}^T\left(D_{RT} + D_{RT}^T\right)V_{T0} \\
&\quad + V_{TR}^T E_T V_{TR} + 2V_{TR}^T D_{Re}\mathrm{T}' + 2V_{TR}^T\left(D_{RT} + D_{RT}^T\right)V_{T0} + V_{T0}^T D_{RR} V_{T0}
\end{aligned} \tag{35}
$$

where the newly defined matrices are

$$
\begin{aligned}
D_{Re} &= \left\langle\left\langle\left[\Gamma_{RT}S\right]^T K e_1\right\rangle\right\rangle \\
D_{RT} &= \left\langle\left\langle\left[\Gamma_{RT}S\right]^T K\left[\Gamma_T S\right]\right\rangle\right\rangle \\
D_{RR} &= \left\langle\left\langle\left[\Gamma_{RT}S\right]^T K\left[\Gamma_{RT}S\right]\right\rangle\right\rangle
\end{aligned} \tag{36}
$$

The leading terms with respect to the unknown V_{TR} from Eq. (35) are

$$
2U_{T1}^{*} = V_{TR}^T E_T V_{TR} + 2V_{TR}^T D_R \mathrm{T}' \tag{37}
$$

with $D_R = D_{Re} + \left(D_{RT} + D_{RT}^T\right)\bar{V}_{T0}$. It is noted that $\sqrt{g}$ contains k_α, and it is should be expanded in the asymptotic analysis so that

$$
E_T = \left\langle\left[\Gamma_T S\right]^T K\left[\Gamma_T S\right]\right\rangle + \left\langle\left[\Gamma_T S\right]^T K\left[\Gamma_T S\right]\left(x_3 k_2 - x_2 k_3\right)\right\rangle \tag{38}
$$

For simplicity of notation, we continue to use E_T in derivation with the understanding that such expansion are actually carried out in the numerical implementation.

Minimizing the leading terms in Eq. (37) subject to the constraint in Eq. (15), we can obtain the thermal warping function in the following form

$$
V_{TR} = \bar{V}_{TR}\mathrm{T}' \tag{39}
$$

Having obtained $\bar{V}_{T0}$ and $\bar{V}_{TR}$, we can approximate the original functional in Eq. (9) using the following 1D functional

$$
\prod\nolimits_1 = \int_0^l \left[U_{T1} - \left(\left\langle\left\langle Q\right\rangle\right\rangle + \oint_{\partial\Omega}\bar{q}ds\right)\Gamma\right]dx_1 - \left\langle\bar{q}_e\mathrm{T}\right\rangle\Big|_{x_1=l} - \left\langle\bar{q}_e\mathrm{T}\right\rangle\Big|_{x_1=0} \tag{40}
$$

where

$$
\begin{aligned}
U_{T1} &= \frac{1}{2}\left(\bar{V}_{T0}^T D_T + \bar{K} + \bar{V}_{T0}^T D_R + \bar{V}_{T0}^T D_{Re} + \bar{V}_{T0}^T D_{RR}\bar{V}_{T0} + \bar{V}_{TR}^T D_R\right)\mathrm{T}'^2 \\
&\equiv \frac{1}{2}\bar{K}_R\mathrm{T}'^2
\end{aligned} \tag{41}
$$

3.3 Dimensional reduction of case 2

3.3.1 Zeroth-order approximation

The temperature field of this case is provided in Eq. (16) and can be discretized as

$$T(x_1, x_2, x_3) = w_T(x_1, x_2, x_3) = S(x_2, x_3)V_T(x_1) \tag{42}$$

For simplicity of illustration, let us assume Q, $\bar{q}$ and $\bar{q}_e$ vanish, then the zeroth-order approximation of the thermal warping function should be solved from minimizing the following functional

$$2\mathcal{U}_{T0} = V_{T0}^T E_T V_{T0} \tag{43}$$

with some values of V_{T0} prescribed at certain nodes. As long as there is at least one point having prescribed temperature, the thermal warping function can be solved uniquely.

3.3.2 First-order approximation

For the refined model with respect to initial twist and curvatures based on the first-order approximation, we expand the unknown thermal warping function V_T asymptotically as we did for thermal load case 1 in Eq. (34) where $V_{TR} \sim O(\breve{h}\mathcal{T}')$ and it should be zero at the points where the temperature is prescribed as the prescribed condition has already been satisfied by V_{T0}. Following what we did before, we obtain the following equation to solve for the first-order thermal warping

$$E_T V_{TR} = -\left(D_{RT}^T + D_{RT} + E_T\right)V_{T0} \tag{44}$$

Here it is noted that the zero constraints for V_{TR} at the prescribed points should be introd uced to solve the linear system. The prescribed temperature at certain nodes can be consid ered as single-point constraint that sets a single degree of freedom to a known value. The solution procedure of this kind of problem can be found in a typical textbook of finite ele ment method such as by Cook *et al*. (2001).

3.4 Recovery of 3D thermal field

Thus far, we have obtained a generalized beam model for heat conduction analysis of thermal load case 1. The generalized heat conduction coefficients $\bar{K}_0$ and $\bar{K}_R$ can be used as an input for a 1D beam analysis to calculate the global thermal behavior. In other words, $\mathcal{T}(x_1)$ can be solved using Eq. (25) or Eq. (40). However, only predicting the global behavior is not sufficient, and the original 3D results should be recovered for detailed analysis. The recovery procedure of heat conduction analysis can be summarized as

1. Using Eq. (25) or Eq. (40) to find $\mathcal{T}(x_1)$;
2. Using Eq. (21) along with Eq. (34) to calculate the thermal warping function;
3. Using Eq. (14) to obtain the 3D temperature field;
4. Having the 1D temperature $\mathcal{T}(x_1)$ and warping functions $\bar{V}_{T0}$ and $\bar{V}_{TR}$, it is straight forward to obtain the 3D temperature gradient using Eq. (17) as

$$\nabla T = \left[e_1 + \left(\Gamma_T S + \Gamma_{RT} S\right)\left(\bar{V}_{T0} + \bar{V}_{TR}\right)\right]\mathcal{T}' \tag{45}$$

and 3D heat flux within the beam using

$$\begin{Bmatrix} q_1 \\ q_2 \\ q_3 \end{Bmatrix} = -K\nabla T \tag{46}$$

The recovery of temperature field for thermal load case 2 is easier than that for case 1. Since there is no 1D variables like $\mathbb{T}(x_1)$, the temperature can be obtained directly from Eq. (42) along with the solution of thermal warping functions in Eqs. (43) and (44).

4. Thermoelastic analysis

4.1 Governing functional

The kinematics of the composite beam will remain the same as the isothermal condition. As derived in Yu *et al*. (2002), the 3D strain field can be expressed as

$$\Gamma = \Gamma_h w + \Gamma_\epsilon \bar{\epsilon} + \Gamma_R w + \Gamma_l w' \tag{47}$$

where Γ is the column matrix of engineering strains arranged as

$$\Gamma = [\Gamma_{11} \quad 2\Gamma_{12} \quad 2\Gamma_{13} \quad \Gamma_{22} \quad 2\Gamma_{23} \quad \Gamma_{33}]^T \tag{48}$$

$\bar{\epsilon} = \lfloor \bar{\gamma}_{11} \; \bar{\kappa}_1 \; \bar{\kappa}_2 \; \bar{\kappa}_3 \rfloor$ contains the generalized 1D strain measures for a classical beam model. The operators in Eq. (47) are defined as

$$\Gamma_h = \begin{bmatrix} 0 & 0 & 0 \\ \partial_2 & 0 & 0 \\ \partial_3 & 0 & 0 \\ 0 & \partial_2 & 0 \\ 0 & \partial_3 & \partial_2 \\ 0 & 0 & \partial_3 \end{bmatrix} \tag{49}$$

$$\Gamma_\varepsilon = \frac{1}{\sqrt{g}} \begin{bmatrix} 1 & 0 & x_3 & -x_2 \\ 0 & -x_3 & 0 & 0 \\ 0 & x_2 & 0 & 0 \\ 0 & 0 & 0 & 0 \\ 0 & 0 & 0 & 0 \\ 0 & 0 & 0 & 0 \end{bmatrix} \tag{50}$$

$$\Gamma_R = \frac{1}{\sqrt{g}}\begin{bmatrix} k_1(x_3\partial_2 - x_2\partial_3) & -k_3 & k_2 \\ k_3 & k_1(x_3\partial_2 - x_2\partial_3) & -k_1 \\ -k_2 & k_1 & k_1(x_3\partial_2 - x_2\partial_3) \\ 0 & 0 & 0 \\ 0 & 0 & 0 \\ 0 & 0 & 0 \end{bmatrix} \tag{51}$$

$$\Gamma_l = \frac{1}{\sqrt{g}}\begin{bmatrix} 1 & 0 & 0 \\ 0 & 1 & 0 \\ 0 & 0 & 1 \\ 0 & 0 & 0 \\ 0 & 0 & 0 \\ 0 & 0 & 0 \end{bmatrix} \tag{52}$$

The thermoelastic energy of an elastic solid can be described using the Helmholtz free energy. For beam structures, it can be written as

$$U_A = \int_0^l \mathrm{U}_A dx_1 \tag{53}$$

U_A is the energy density defined as

$$\mathrm{U}_A = \left\langle\left\langle \frac{1}{2}\Gamma^T \mathrm{D}\Gamma - \Gamma^T \mathrm{D}\alpha\Delta T \right\rangle\right\rangle \tag{54}$$

where ΔT is the difference between the temperature in the structure and the reference temperature when the beam is stress free, D is the 6×6 material matrix, which contains elements of the fourth-order elasticity tensor expressed in the triad $\mathbf{b}_i$, and α is a 6×1 column matrix containing the components of the second-order thermal expansion tensor expressed in the triad $\mathbf{b}_i$. These matrices are in general fully populated. It needs to be pointed out that Eq. (54) is based on small strain assumption and small temperature change assumption and the material properties are independent of temperature change. However, it can be directly generalized to handle finite temperature change and account for the dependency of material properties which will be shown later.

4.2 Dimensional reduction

4.2.1 Zeroth-order approximation - generalized Euler-Bernoulli model

For the zeroth-order approximation, we keep the terms up to $O(\nu\breve{\varepsilon}^2)$, where ν and $\breve{\varepsilon}$ denote the order of elastic constants and 1D generalized strains, respectively. The Helmholtz free

energy per unit span can be written as

$$\mathrm{U}_{A0} = \left\langle \left\langle \frac{1}{2}\Gamma_0^T \mathrm{D}\Gamma_0 - \Gamma_0^T \mathrm{D}\alpha\Delta T \right\rangle \right\rangle \tag{55}$$

with Γ_0 obtained from Eq. (47) by dropping the last two higher order terms as

$$\Gamma_0 = \Gamma_a w + \Gamma_\epsilon \bar{\epsilon} \tag{56}$$

The unknown 3D warping functions $w_i(x_1, x_2, x_3)$ can be solved from the following much simpler variation statement

$$\delta \mathrm{U}_{A0} = 0 \tag{57}$$

along with the constraints in Eq. (7). Similarly, to deal with arbitrary cross-sectional geometry and anisotropic materials, we need to discretize the mechanical warping field as

$$w(x_1, x_2, x_3) \;=\; S(x_2, x_3)\; V(x_1) \tag{58}$$

with $S(x_2, x_3)$ representing the matrix of finite element shape functions, and V as a column matrix of the nodal values of the warping functions over the cross-section.

Substituting Eq. (56) along with Eq. (58) into Eq. (55), one can express the zeroth-order Helmholtz free energy in discretized form as

$$2U_{A0} = V^T E V + 2V^T D_{a\epsilon}\bar{\epsilon} + \bar{\epsilon}^T D_{\epsilon\epsilon}\bar{\epsilon} - 2\left(V^T \alpha_a + \bar{\epsilon}^T \alpha_\epsilon\right) \tag{59}$$

where the newly introduced matrices carry information of both the geometry of the cross-section and material properties, defined as

$$\begin{aligned} E &= \left\langle \left\langle [\Gamma_a S]^T D [\Gamma_a S] \right\rangle \right\rangle \qquad \alpha_a = \left\langle \left\langle [\Gamma_a S]^T D\alpha\Delta T \right\rangle \right\rangle \\ D_{a\epsilon} &= \left\langle \left\langle [\Gamma_a S]^T D\Gamma_\epsilon \right\rangle \right\rangle \qquad \alpha_\epsilon = \left\langle \left\langle [\Gamma_\epsilon]^T D\alpha\Delta T \right\rangle \right\rangle \\ D_{\epsilon\epsilon} &= \left\langle \left\langle [\Gamma_\epsilon]^T D [\Gamma_\epsilon] \right\rangle \right\rangle \end{aligned} \tag{60}$$

Substituting Eq. (58) into Eq. (7), we can express the constraints in a discretized form as

$$V^T D_c = 0 \tag{61}$$

with $D_c^T = \langle \Gamma_c S \rangle$. We also denote the corresponding kernel matrix of E as Ψ so that $E\Psi = 0$.

Now the problem has been transformed to numerical minimization of Eq. (59) subject to constraints in Eq. (61). The Euler-Lagrange equation for this problem can be obtained by usual procedure of calculus of variations with the aid of Lagrange multipliers Λ as follows

$$EV + D_{a\epsilon}\bar{\epsilon} - \alpha_a = D_c \Lambda \tag{62}$$

Multiplying both sides by Ψ^T and considering the properties of the kernel matrix Ψ, one calculates the Lagrange multiplier Λ as

$$\Lambda = \left(\psi^T D_c\right)^{-1} \psi^T \left(D_{a\in}\bar{\in} - \alpha_a\right) \tag{63}$$

It is clear that Λ vanishes because $\psi^T D_{a\in} = \left\langle\left\langle (\Gamma_a S\psi)^T D\Gamma_\in \right\rangle\right\rangle = 0$, similarly $\Psi^T \alpha_a = 0$, which implies that the constraints will not affect the minimum value of U_{A0}. Then the linear system in Eq. (62) becomes

$$EV = -D_{a\in}\bar{\in} + \alpha_a \tag{64}$$

There exists a unique solution linearly independent of Ψ, the null space of E, for V because the right-hand-side of Eq. (64) is orthogonal to the null space. Because of the uniqueness of the solution, the linear system in Eq. (64) can be solved by letting the numerical algorithm to determine where the singularities are and properly remove the singularities of the coefficient matrix. Let us denote the solution of Eq. (64) obtained this way as V^*, the complete solution can be written as

$$V = V^* + \Psi\lambda \tag{65}$$

where λ can be determined by Eq. (61) as

$$\lambda = -\left(\Psi^T D_c\right)^{-T} D_c^T V^* \tag{66}$$

Hence the final solution minimizing the functional in Eq. (59) and satisfying the constraints in Eq. (61) is

$$V = \left[\Delta - \psi\left(\psi^T D_c\right)^{-T} D_c^T\right] V^* = \hat{V}_0 \bar{\in} + V_{t0} \equiv V_0 \tag{67}$$

where V_{t0} is the mechanical warping caused by the applied temperature field.

Substituting Eq. (67) back into Eq. (59), one can obtain the total energy asymptotically correct up to the $O(\nu\check{o}^2)$ as

$$2U_{A0} = \bar{\in}^T \left(\hat{V}_0^T D_{a\in} + D_{\in\in}\right)\bar{\in} - 2\bar{\in}^T\left[\alpha_\in + \frac{1}{2}\left(\hat{V}_0^T \alpha_a - D_{a\in}^T V_{t0}\right)\right] \tag{68}$$

Note the quadratic terms associated with temperature $V_{t0}^T \alpha_a$ and $V_{t0}^T E V_{t0}$ are dropped because they will not contribute to the corresponding 1D thermoelastic beam model. This is the asymptotically correct energy for a beam without correction for initial curvature and twist. This energy can be written in an explicit matrix form as

$$2U_{A0} = \begin{Bmatrix} \bar{\gamma}_{11} \\ \bar{\kappa}_1 \\ \bar{\kappa}_2 \\ \bar{\kappa}_3 \end{Bmatrix}^T \begin{bmatrix} \bar{S}_{11} & \bar{S}_{12} & \bar{S}_{13} & \bar{S}_{14} \\ \bar{S}_{12} & \bar{S}_{22} & \bar{S}_{23} & \bar{S}_{24} \\ \bar{S}_{13} & \bar{S}_{23} & \bar{S}_{33} & \bar{S}_{34} \\ \bar{S}_{14} & \bar{S}_{24} & \bar{S}_{34} & \bar{S}_{44} \end{bmatrix} \begin{Bmatrix} \bar{\gamma}_{11} \\ \bar{\kappa}_1 \\ \bar{\kappa}_2 \\ \bar{\kappa}_3 \end{Bmatrix} - 2 \begin{Bmatrix} \bar{\gamma}_{11} \\ \bar{\kappa}_1 \\ \bar{\kappa}_2 \\ \bar{\kappa}_3 \end{Bmatrix}^T \begin{bmatrix} f_1^t \\ m_1^t \\ m_2^t \\ m_3^t \end{bmatrix} \tag{69}$$

which implies a 1D constitutive model of the following form

$$\begin{bmatrix} F_1 \\ M_1 \\ M_2 \\ M_3 \end{bmatrix} = \begin{bmatrix} \bar{S}_{11} & \bar{S}_{12} & \bar{S}_{13} & \bar{S}_{14} \\ \bar{S}_{12} & \bar{S}_{22} & \bar{S}_{23} & \bar{S}_{24} \\ \bar{S}_{13} & \bar{S}_{23} & \bar{S}_{33} & \bar{S}_{34} \\ \bar{S}_{14} & \bar{S}_{24} & \bar{S}_{34} & \bar{S}_{44} \end{bmatrix} \begin{Bmatrix} \bar{\gamma}_{11} \\ \bar{\kappa}_1 \\ \bar{\kappa}_2 \\ \bar{\kappa}_3 \end{Bmatrix} - \begin{bmatrix} f_1^t \\ m_1^t \\ m_2^t \\ m_3^t \end{bmatrix} \tag{70}$$

where F_1 is the axial stress resultant conjugate to the extensional strain $\bar{\gamma}_{11}$ and M_i are the moment resultants conjugate to the twists and curvatures $\bar{\kappa}_i$, *i.e.*,

$$F_1 = \frac{\partial \mathrm{U}_{A0}}{\partial \bar{\gamma}_{11}} \qquad M_i = \frac{\partial \mathrm{U}_{A0}}{\partial \bar{\kappa}_i} \tag{71}$$

This model can be considered as a generalized Euler-Bernoulli beam model while we have not used any *ad hoc* kinematic assumptions. Next we will construct a refined thermoelastic beam model to capture the transverse shear effects as well as the effects due to initial twist and curvatures.

4.2.2 First-order approximation

For the refined modeling, we keep terms up to $O\left(v \breve{\in}^2 \breve{h}^2\right)$ in the expression of the Helmholtz free energy. Perturbing the warping functions to be

$$V = V_0 + V_1 = \hat{V}_0 \bar{\in} + V_{t0} + V_1 \tag{72}$$

Substituting Eq. (72) into Eq. (58), then into Eq. (47), and finally into Eq. (54), we obtain the following functional after neglecting terms higher than $O(v \breve{\in}^2 \breve{h}^2)$

$$\begin{aligned} 2U_{A1} =& \bar{\in}^T (\hat{V}_0^T D_{a\in} + D_{\in\in}) \bar{\in} - 2\bar{\in}^T \left[\alpha_\in + \frac{1}{2} \left(\hat{V}_0^T \alpha_a - D_{a\in}^T V_{t0} \right) \right] \\ &+ 2V_0^T D_{aR} V_0 + 2V_0^T D_{al} V_0' + 2V_0^T D_{R\in} \bar{\in} + 2V_0'^T D_{le} \bar{\in} - 2V_0'^T \alpha_l - 2V_0^T \alpha_R \\ &+ V_1^T E V_1 + 2V_1^T (D_{aR} V_0 + D_{aR}^T V_0 + D_{R\in} \bar{\in}) + 2V_1^T D_{al} V'_0 + 2V_0^T D_{al} V'_1 \\ &+ 2V_1'^T D_{l\in} \bar{\in} + V_0^T D_{RR} V_0 + 2V_0^T D_{Rl} V_0' + V'^T_0 D_{ll} V_0' - 2V'^T_1 \alpha_l - 2V_1^T \alpha_R \end{aligned} \tag{73}$$

where

$$\begin{aligned} D_{aR} &= \left\langle \left\langle [\Gamma_a S]^T D [\Gamma_R S] \right\rangle \right\rangle & \mathrm{D_{RR}} &= \left\langle \left\langle [\Gamma_R S]^T D [\Gamma_R S] \right\rangle \right\rangle \\ D_{al} &= \left\langle \left\langle [\Gamma_a S]^T D [\Gamma_l S] \right\rangle \right\rangle & \mathrm{D_{ll}} &= \left\langle \left\langle [\Gamma_l S]^T D [\Gamma_l S] \right\rangle \right\rangle \\ D_{l\in} &= \left\langle \left\langle [\Gamma_l S]^T D [\Gamma_\in] \right\rangle \right\rangle & \mathrm{D_{R\in}} &= \left\langle \left\langle [\Gamma_R S]^T D [\Gamma_\in] \right\rangle \right\rangle \\ D_{Rl} &= \left\langle \left\langle [\Gamma_R S]^T D [\Gamma_l S] \right\rangle \right\rangle & \alpha_l &= \left\langle \left\langle [\Gamma_l S]^T D \alpha \Delta T \right\rangle \right\rangle \\ \alpha_R &= \left\langle \left\langle [\Gamma_R S]^T D \alpha \Delta T \right\rangle \right\rangle \end{aligned} \tag{74}$$

As we are interested in the interior solution for the beam without consideration of edge effects, we can integrate by parts to get rid of the derivatives of the warping V_1' and neglect the boundary terms. The leading terms (without the constant terms) of Eq. (73) are

$$2U_{A1}^{*} = V_1^T E V_1 + 2V_1^T D_R \bar{\epsilon} + 2V_1^T D_S \bar{\epsilon}' + 2V_1^T (D_{RT} D_{ST}) \tag{75}$$

where

$$D_R = D_{aR} V_0 + D_{aR}^T V_0 + D_{R\epsilon} \tag{76}$$

$$D_S = D_{al} V_0 - D_{al}^T V_0 - D_{l\epsilon} \tag{77}$$

$$\mathrm{D}_{RT} = \left(D_{aR}^T + D_{aR} \right) V_{t0} - \alpha_R \tag{78}$$

$$D_{ST} = \left(D_{al} - D_{al}^T \right) V_{t0}' + \alpha_l' \tag{79}$$

Similar to the zeroth-order warping, the first-order warping could be solved as

$$V_1 = V_{1R} \bar{\epsilon} + V_{1S} \bar{\epsilon}' + V_{1T} \tag{80}$$

Using Eq. (80), the second-order asymptotically correct Helmholtz free energy can now be obtained from Eq. (54) as

$$2U_{Al} = \bar{\epsilon}^T A \bar{\epsilon} + 2\bar{\epsilon}^T B \bar{\epsilon}' + \bar{\epsilon}'^T C \bar{\epsilon}' + 2\bar{\epsilon}^T D \bar{\epsilon}'' - 2\bar{\epsilon}^T F_{t1} - 2\bar{\epsilon}'^T F_{t2} - 2\bar{\epsilon}''^T F_{t3} \tag{81}$$

Where

$$\begin{aligned}
A &= \hat{V}_0^T D_{a\epsilon} + D_{\epsilon\epsilon} + \hat{V}_0^T (D_{aR} + D_{aR}^T + D_{RR}) \hat{V}_0 + 2\hat{V}_0^T D_{R\epsilon} + V_{1R}^T D_R \\
B &= \hat{V}_0^T (D_{al} + D_{Rl}) \hat{V}_0 + D_{l\epsilon}^T \hat{V}_0 + (\hat{V}_0^T D_{al} + D_{l\epsilon}^T) V_{1R} + \frac{1}{2} (D_R^T V_{1S} + V_{1R}^T \bar{D}_S) \\
C &= V_{1S}^T \bar{D}_S + \hat{V}_0^T D_{ll} \hat{V}_0 \\
D &= (D_{l\epsilon}^T + \hat{V}_0^T D_{al}) V_{1S} \\
F_{t1} &= N_T - (D_R^T + \hat{V}_0^T D_{RR}) V_{t0} - (\hat{V}_0^T D_{al} + D_{l\epsilon}^T + \hat{V}_0^T D_{Rl}) V_{t0}' - \frac{1}{2} D_R^T V_{1T} \\
&\quad - (\hat{V}_0^T D_{al} + D_{l\epsilon}^T) V_{1T}' - \frac{1}{2} V_{1R}^T (D_{RT} + \bar{D}_{ST}) + \hat{V}_0^T \alpha_R \\
F_{t2} &= (\hat{V}_0^T + \hat{V}_{1R}^T) \alpha_l - (\hat{V}_0^T D_{al}^T + \hat{V}_{1R}^T D_{al}^T + \hat{V}_0^T D_{Rl}^T) V_{t0} - \frac{1}{2} \bar{D}_S^T V_{1T} \\
&\quad - \hat{V}_0^T D_{ll} V_{t0}' - \frac{1}{2} V_{1S}^T (D_{RT} + \bar{D}_{ST}) \\
F_{t3} &= -V_{1S}^T D_{al}^T V_{t0} + V_{1S}^T \alpha_l
\end{aligned} \tag{82}$$

with

$$
\begin{aligned}
N_T &= \alpha_{\in} + \frac{1}{2}\hat{V}_0^T \alpha_a - D_{a\in}^T V_{t0} \\
\overline{D}_S &= (D_{al} + D_{al}^T)\hat{V}_0 + D_{l\in} \\
\overline{D}_{ST} &= (D_{al} + D_{al}^T)V_{t0}^{'} - \alpha_l^{'}
\end{aligned}
\tag{83}
$$

4.2.3 Transformation to a generalized Timoshenko model

The energy of the form in Eq. (81) is not convenient for engineering applications because it involves derivatives of the 1D generalized strains. To get rid of these derivatives, we can transform this asymptotically correct energy expression to a generalized Timoshenko model following the procedure in Yu *et al*. (2012).

The key to the energy transformation is to find expressions for , $\overline{\in}, \overline{\in}'$ and $\overline{\in}''$ in terms of $\in$ and γ_s. Following the procedure in Yu *et al*. (2012), we can finally express the energy up to the second order as

$$
2U_{AT} = \in^T X \in + 2 \in^T Y\gamma_s + \gamma_s^T G\gamma_s - 2 \in^T F_1^t - 2\gamma_s^T F_2^t \tag{84}
$$

where $F_1^t = \left[\mathrm{F}_1^{\,t} \ \mathrm{M}_1^{\,t} \ \mathrm{M}_2^{\,t} \ \mathrm{M}_3^{\,t} \right]^T$ and $F_2^t = \left[\mathrm{F}_2^{\,t} \ \mathrm{F}_3^{\,t} \right]^T$. We can rewrite this model in an explicit matrix form as

$$
2\mathrm{U}_A = \begin{Bmatrix} \gamma_{11} \\ 2\gamma_{12} \\ 2\gamma_{13} \\ \kappa_1 \\ \kappa_2 \\ \kappa_3 \end{Bmatrix}^T \begin{bmatrix} S_{11} & S_{12} & S_{13} & S_{14} & S_{15} & S_{16} \\ S_{12} & S_{22} & S_{23} & S_{24} & S_{25} & S_{26} \\ S_{13} & S_{23} & S_{33} & S_{34} & S_{35} & S_{36} \\ S_{14} & S_{24} & S_{34} & S_{44} & S_{45} & S_{46} \\ S_{15} & S_{25} & S_{35} & S_{45} & S_{55} & S_{56} \\ S_{16} & S_{26} & S_{36} & S_{46} & S_{56} & S_{66} \end{bmatrix} \begin{Bmatrix} \gamma_{11} \\ 2\gamma_{12} \\ 2\gamma_{13} \\ \kappa_1 \\ \kappa_2 \\ \kappa_3 \end{Bmatrix} - 2 \begin{Bmatrix} \gamma_{11} \\ 2\gamma_{12} \\ 2\gamma_{13} \\ \kappa_1 \\ \kappa_2 \\ \kappa_3 \end{Bmatrix}^T \begin{Bmatrix} \mathrm{F}_1^{\,t} \\ \mathrm{F}_2^{\,t} \\ \mathrm{F}_3^{\,t} \\ \mathrm{M}_1^{\,t} \\ \mathrm{M}_2^{\,t} \\ \mathrm{M}_3^{\,t} \end{Bmatrix} \tag{85}
$$

which implies the following 1D constitutive model

$$
\begin{bmatrix} F_1 \\ F_2 \\ F_3 \\ M_1 \\ M_2 \\ M_3 \end{bmatrix} = \begin{bmatrix} S_{11} & S_{12} & S_{13} & S_{14} & S_{15} & S_{16} \\ S_{12} & S_{22} & S_{23} & S_{24} & S_{25} & S_{26} \\ S_{13} & S_{23} & S_{33} & S_{34} & S_{35} & S_{36} \\ S_{14} & S_{24} & S_{34} & S_{44} & S_{45} & S_{46} \\ S_{15} & S_{25} & S_{35} & S_{45} & S_{55} & S_{56} \\ S_{16} & S_{26} & S_{36} & S_{46} & S_{56} & S_{66} \end{bmatrix} \begin{Bmatrix} \gamma_{11} \\ 2\gamma_{12} \\ 2\gamma_{13} \\ \kappa_1 \\ \kappa_2 \\ \kappa_3 \end{Bmatrix} - \begin{Bmatrix} \mathrm{F}_1^{\,t} \\ \mathrm{F}_2^{\,t} \\ \mathrm{F}_3^{\,t} \\ \mathrm{M}_1^{\,t} \\ \mathrm{M}_2^{\,t} \\ \mathrm{M}_3^{\,t} \end{Bmatrix} \tag{86}
$$

where $\lfloor F_1 \ F_2 \ F_3 \rfloor^T$ are the stress resultants conjugate to the force strain $\lfloor \gamma_{11} \quad 2\gamma_{12} \quad 2\gamma_{13} \rfloor^T$ and $\lfloor M_1 \ M_2 \ M_3 \rfloor^T$ are the moment resultants conjugate to the moment strains $\lfloor \kappa_1 \ \kappa_2 \ \kappa_3 \rfloor^T$; $\lfloor F_1^t \ F_2^t \ F_3^t \rfloor^T$ and $\lfloor M_1^t \ M_2^t \ M_3^t \rfloor^T$ are temperature induced resultants corresponding to the force strains and moment strains, respectively.

4.3 Recovery of 3D mechanical field

In this section, we are going to recover the original 3D results based on the developed 1D constitutive models.

For the generalized thermoelastic Timoshenko model of an initially curved and twisted beam, the warping function that is asymptotically correct up to the order of $\tilde{h} \sim h/R \sim h/l$ can be expressed as

$$w(x_1, x_2, x_3) = S(\hat{V}_0 + V_{1R})\,\overline{\in} + SV_{1S}\,\overline{\in}' + S(V_{t0} + V_{1T}) \tag{87}$$

From Eq. (5) and Eq. (1), we can calculate the 3D displacement field as

$$\bar{u}_i(x_1, x_2, x_3) = u_i(x_1) + x_\alpha\left[C^{Tb}_{\alpha i}(x_1) - \delta_{\alpha i}\right] + C^{Tb}_{ji} w_j(x_1, x_2, x_3) \tag{88}$$

where $\bar{u}_i$ are the 3D displacements, u_i the 1D beam displacements, and C^{Tb}_{ij} the components of the direction cosine matrix representing the finite rotation from triad $\mathbf{b}_i$ to triad $\mathbf{T}_i$.

The 3D strain field can be recovered by substituting 1D strain measures, cross-sectional warping and their derivatives into Eq. (47). Substituting Eq. (87) into Eq. (47), we obtain

$$\begin{aligned}\Gamma = &\left[(\Gamma_a + \Gamma_R)S(\hat{V}_0 + V_{1R}) + \Gamma_\in\right]\overline{\in} \\ &+ \left[(\Gamma_a + \Gamma_R)SV_{1S} + \Gamma_l S(\hat{V}_0 + V_{1R})\right]\overline{\in}' \\ &+ \Gamma_l SV_{1S}\,\overline{\in}'' \\ &+ (\Gamma_a + \Gamma_R)S(V_{t0} + V_{1T}) + \Gamma_l S(V_{t0}^{'} + V_{1T}^{'})\end{aligned} \tag{89}$$

Finally, the stress can be obtained from the 3D constitutive relations based on the Helmholtz free energy in Eq. (54) so that

$$\sigma = D\Gamma - D\alpha\Delta T \tag{90}$$

where σ is a column matrix containing σ_{ij} as

$$\sigma = \left\lfloor \sigma_{11}\ \sigma_{12}\ \sigma_{13}\ \sigma_{22}\ \sigma_{23}\ \sigma_{33}\right\rfloor^T \tag{91}$$

4.4 Thermoelastic beam modeling under large temperature changes

To relax the assumption of small temperature changes, we need to derive a Helmholtz free energy suitable for materials with temperature dependent properties and experiencing finite temperature changes as what has been done in Teng *et al*. (2012) for micromechanics modeling of heterogeneous materials. Although the derivation is similar, some of the derivations in Teng *et al*. (2012) is repeated here for the paper to be self contained.

The Helmholtz free energy density $f(\in_{ij}, T)$ is a function of strain field $\in_{ij}$ and the absolute temperature T. Let us not put any restriction on T but assuming $\in_{ij}$ to be small, then we can carry out a Taylor expansion of $f(\in_{ij}, T)$ in terms of the small strain field, $\in_{ij}$, as

$$f(\in_{ij},T) = f(0,T) + \in_{ij} \left.\frac{\partial f(\in_{ij},T)}{\partial \in_{ij}}\right|_{\in_{ij}=0} + \frac{1}{2} \in_{ij} \in_{kl} \left.\frac{\partial^2 f(\in_{ij},T)}{\partial \in_{ij} \partial \in_{kl}}\right|_{\in_{ij}=0} \tag{92}$$

Here only up to the quadratic terms of the strain field are kept due the assumption of small strains. As the constant term $f(0,T)$ will not affect our thermoelastic analysis (Boley and Weiner 1997), the constant term $f(0,T)$ is dropped. We know $\sigma_{ij} = \dfrac{\partial f}{\partial \in_{ij}}$, that is

$$\sigma_{ij} = C_{ijkl}(T) \in_{kl} + l_{ij}(T) \tag{93}$$

with $C_{ijkl}(T) = \left.\dfrac{\partial^2 f(\in_{ij},T)}{\partial \in_{ij} \partial \in_{kl}}\right|_{\in_{ij}} = 0$ as the fourth-order elasticity tensor and $l_{ij}(T) = \left.\dfrac{\partial f(\in_{ij},T)}{\partial \in_{ij}}\right|_{\in_{ij}} = 0$ as the second-order thermal stress tensor. We can also rewrite the stress-strain relations as

$$\in_{ij} = S_{ijkl}(T)\sigma_{kl} + m_{ij}(T) \tag{94}$$

with S_{ijkl} as the fourth-order compliance tensor and m_{ij} as the second-order thermal strain tensor and we have $m_{ij} = -S_{ijkl} l_{kl}$. The coefficients of thermal expansion, α_{ij} , as a function of stress field and temperature, is defined as

$$\alpha_{ij} = \left.\frac{\partial \in_{ij}}{\partial T}\right|_{\sigma_{ij}=\text{constant}} \tag{95}$$

Then from Eqs. (94) and (95), we have

$$\alpha_{ij} = \frac{dS_{ijkl}}{dT}\sigma_{kl} + \frac{dm_{ij}}{dT} \tag{96}$$

From Eq. (96), we have

$$\alpha_{ij}(0,T) = \frac{dm_{ij}}{dT} \tag{97}$$

where we can obtain

$$m_{ij} = \int_{T_0}^{T} \alpha_{ij}(0,\zeta) d\zeta + m_{ij}(T_0) \tag{98}$$

Note here $\alpha_{kl}(0,T)$ are the stress-free coefficients of thermal expansion which can be measured at a specific temperature T . We normally choose our reference state to be at $T = T_0$ with stress and strain free, which implies $m_{ij}(T_0) = 0$ in view of Eq. (94). Then we can express our thermal strain tensor in a form similar as that we used for small temperature variations

$$m_{ij} = \breve{\alpha}_{ij}(T)\Delta T \tag{99}$$

with

$$\breve{\alpha}_{ij}(T) = \frac{1}{\Delta T}\int_{T_0}^{T_0+\Delta T} \alpha_{ij}(0,\zeta)d\zeta \tag{100}$$

where $\breve{\alpha}_{ij}(T)$ is commonly called as the secant stress-free thermal expansion coefficients. We can also express the thermal stress tensor as

$$l_{ij}(T) = -C_{ijkl}(T)m_{kl}(T) = -C_{ijkl}(T)\breve{\alpha}_{ij}(T)\Delta T \equiv \breve{\beta}_{ij}(T)\Delta T \tag{101}$$

Here, $\breve{\beta}_{ij}(T)$ can be similarly called secant strain-free thermal stress coefficients.

Substituting Eq. (101) into Eq. (92), we have the Helmholtz energy for thermoelastic analysis considering the temperature-dependent material properties without assuming small temperature changes as

$$f(\in_{ij},T) = \frac{1}{2}C_{ijkl}\in_{ij}\in_{kl} + \breve{\beta}_{ij}(T)\in_{ij}\Delta T \tag{102}$$

Given the derivation, current VABS thermoelastic model can be easily extended to incorporate the temperature dependent properties of materials. If temperature change is small, α is the conventional CTE, also known as the tangent or instantaneous CTE. Otherwise, for finite temperature change, one just needs to use the secant CTE, which can be obtained from Eq. (100), in Eq. (54).

5. Numerical examples

The theory developed in the previous chapter has been implemented into the computer program *V*ariational *A*symptotic *B*eam *S*ectional Analysis (VABS). To validate the present model, we have used VABS to analyze several examples and the results are compared with 3D finite element analysis in the commercial software ANSYS.

5.1 Example 1: two-layer beam under thermal load case 1 and convection analysis

The first example is a two-layer angle-ply composite beam with the lay-up angle as $\left[30^\circ/-30^\circ\right]$. The length of the beam is 0.2 m (x_1 direction), the thickness of each layer is 0.01 m (x_3 direction), and the width equals to 0.04 m (x_2 direction). The beam is made of an orthotropic material with thermal conductivities given by $k_{11} = 0.3$ W/(m$^\circ$C), $k_{22} = k_{33} = 0.16$ W/(m$^\circ$C). Three thermal load cases are considered

- Case A: constrained temperature on the end surfaces of the beam such as

$$T_0 = 0^\circ\text{C} \quad T_L = 100^\circ\text{C} \tag{103}$$

- Case B: the constrained temperature in the previous case together with input heat flux

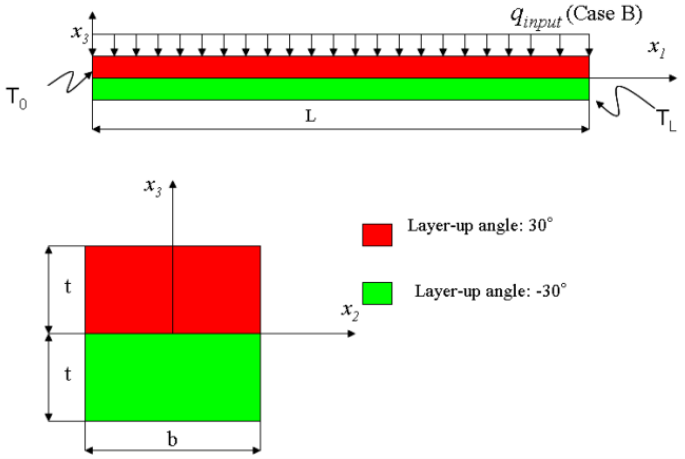

Fig. 3 Sketch of a composite beam used in Example 1

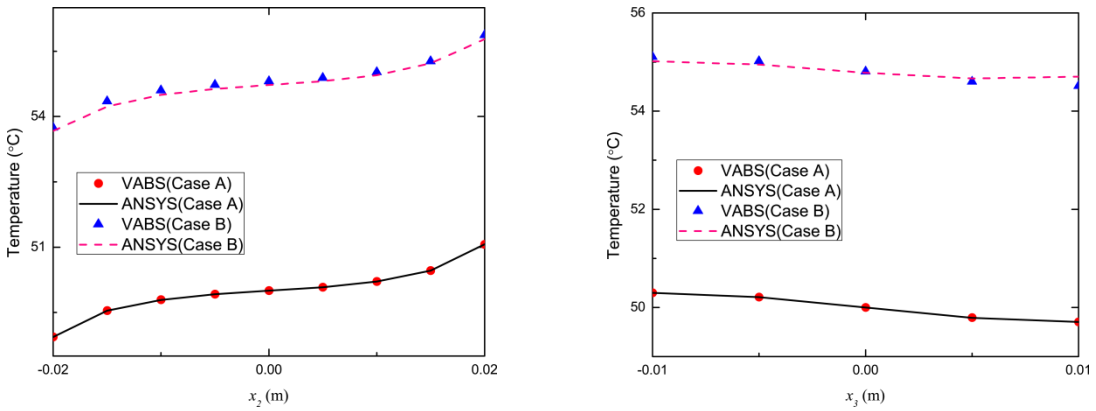

(a) Temperature distribution along width (b) Temperature distribution along thickness

Fig. 4 Recovered temperature field over the cross-section: (a) temperature distribution along the width at $x_3 = -0.005$ m and (b) temperature distribution along the thickness at $x_2 = 0.01$ m.

of 5 W/m^2 in x_3 direction on the top surface of the beam.

- Case C: temperature is prescribed at the left end as $T(x_1 = 0) = 50^\circ$C and the tip is insulated. The ambient temperature is 20°C and the heat transfer coefficient h_c is 2W/m^{2}K.

The geometry and loads of this beam refer to Fig. 3. For VABS analysis, this cross-section is meshed with 32 four-noded quadrilateral elements (eight elements along the width, two elements along the thickness of each layer). SOLID70 thermal elements are used to carry out a thermal analysis in ANSYS with the same cross-sectional mesh and the length is discretized into eight divisions. For comparison, we plot the temperature distribution over the cross-section at $x_1 = 0.1$m along the width and the thickness in Fig. 4(a) and Fig. 4(b), respectively. It can be observed that VABS agrees with ANSYS very well for both cases along the width and the

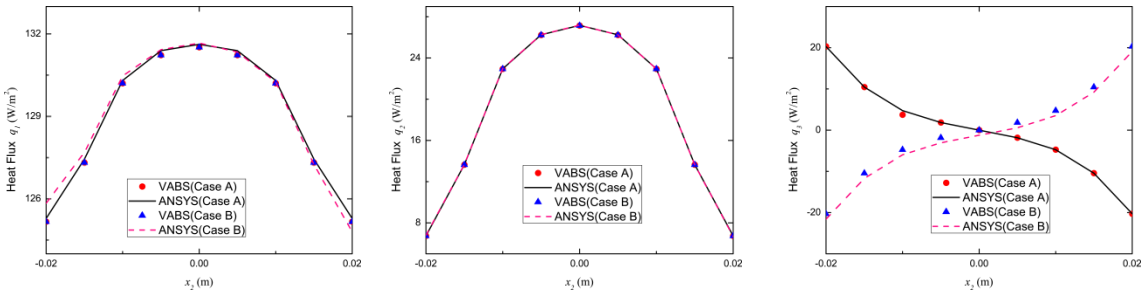

(a) Heat flux q_1 (a) Heat flux q_2 (a) Heat flux q_3

Fig. 5 Recovered heat flux over the cross-section: distributions of heat flux along width at $x_3 = -0.005$ m (a) q_1 ; (b) q_2 and (c) q_3.

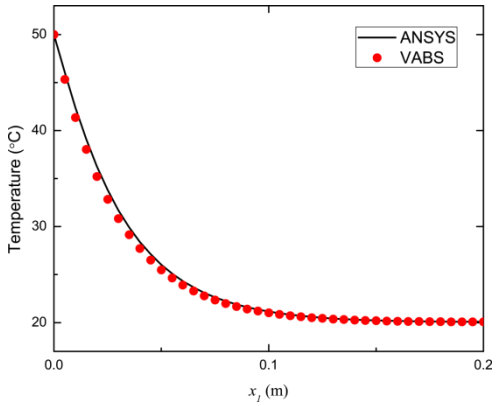

Fig. 6 Temperature distribution along beam axis of Case C

thickness of the cross-section, within differences less than 0.02% and 0.04% for the first and second load case, respectively. In addition to accurately predicting the temperature field, the present model is also able to predict the heat flux within the structure. As shown in Figs. 5(a), 5(b), and 5(c), this model also accurately predicts the heat flux. For the first load case, the error compared with 3D ANSYS analysis is less than 0.1% in predicting the heat flux. For the second load case, the distribution of q_3 has been sharply changed due to the heat flux input on the top surface of the beam. The maximum error between VABS and 3D ANSYS analysis for this case is around 3%.

For Case C, the temperature distribution at the centroid along the beam axis is plotted in Fig.6. Good agreement between results from VABS calculation and those from 3D analysis can be observed.

5.2 Example 2: analysis of a sandwich beam

Sandwich beam structure refers to a special class of composite beams that is fabricatedby attaching two thin but stiff skins, often not identical, to a lightweight but thick core (Wikipedia 2011, Frostig *et al*. 1992). Comparing to the skins, the rigidity of the core is about several orders

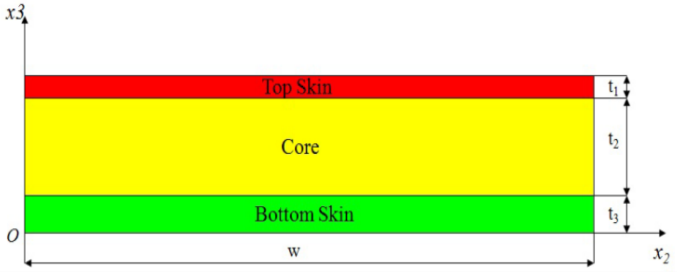

Fig. 7 Sketch of the cross-section of a sandwich beam used in Example 2

Table 1 Material properties and geometric properties of a sandwich beam

Layer	Material Properties	Geometric Properties
Top Skin	E = 59 MPsi, $\nu = 0.14$ $\alpha = 4\times10^{-6}$/K, $k = 80$ W/(m°K)	$t_1 = 0.125$ in. $w = 30$ in.
Core Material 1	E = 0.048 MPsi, $\nu = 0.12$ $\alpha = 1\times10^{-6}$/K, $k = 0.3$ W/(m°K)	$t_2 = 1.5$ in. $w = 30$ in.
Core Material 2	E = 0.004 MPsi, $\nu = 0.49$ $\alpha = 39.9\times10^{-6}$/K, $k = 0.13$ W/(m°K)	$t_2 = 1.5$ in. $w = 30$ in.
Bottom Skin	E = 7.64 MPsi, $\nu = 0.32$ $\alpha_x = 1.6\times10^{-6}$/K, $k = 80$ W/(m°K) $\alpha_y = 28.1\times10^{-6}$/K	$t_3 = 0.25$ in. $w = 30$ in.

lower. But its higher thickness provides the sandwich structure with high bending stiffness with overall low density. A typical application of sandwich structure is thermal protection system. The second example is analysis of a sandwich beam with different configurations under thermal load case 2.

Fig. 7 shows the configuration of the cross-section of the sandwich beam used in the current example. It is a beam of infinity long along x_1 direction and the core can be Material 1 and Material 2, so two cases are analyzed. The first case where Core Material 1 is used is called Case 1, and the second case is called Case 2 where Core Material 2 is used in the beam. The geometric and material properties are listed in Table 1. A temperature of 2000°F is applied at the top surface, and the bottom surface is constrained as 600°F.

The temperature distributions are plotted in Fig. 8(a), and the non-zero stress components are plotted in Figs. 8(b) and 8(c). Although the ratio of rigidity between skin and core materials changing from 1,000 to 10,000, the current model does a pretty good job in predicting thermal and mechanical behavior of the sandwich beam.

5.3 Example 3: thermoelastic analysis of a realistic rotor blade

The authors are not aware of any previous studies on thermoelastic analysis of realistic blade with prediction of the stresses over the entire cross-section, so this example shows that the current

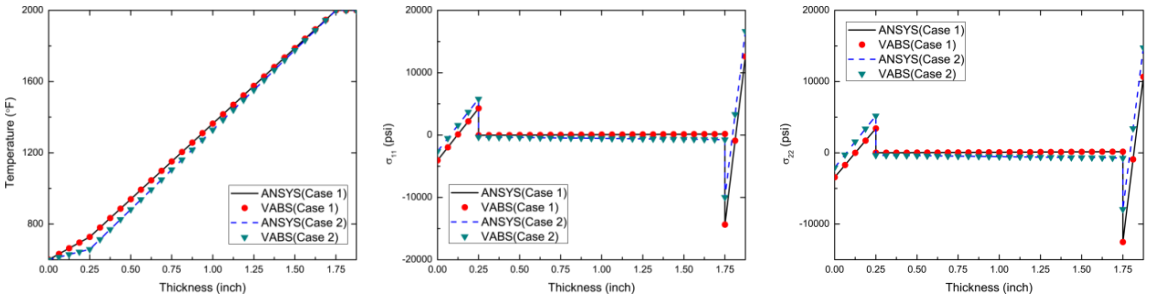

(a) Temperature (a) σ_{11} (a) σ_{22}

Fig. 8 Recovered 3D field over the cross-section: (a) temperature distribution along thickness at $x_2 = \frac{1}{2}w$; (b) distribution of σ_{11} along thickness at $x_2 = \frac{1}{2}w$; and (c) distribution of σ_{22} along thickness at $x_2 = \frac{1}{2}w$

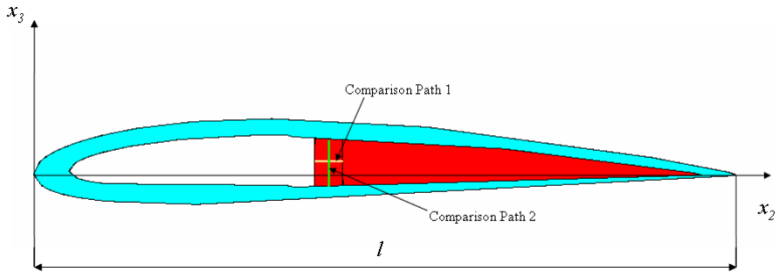

Fig. 9 Sketch of a cross-section for NACA2412 blade

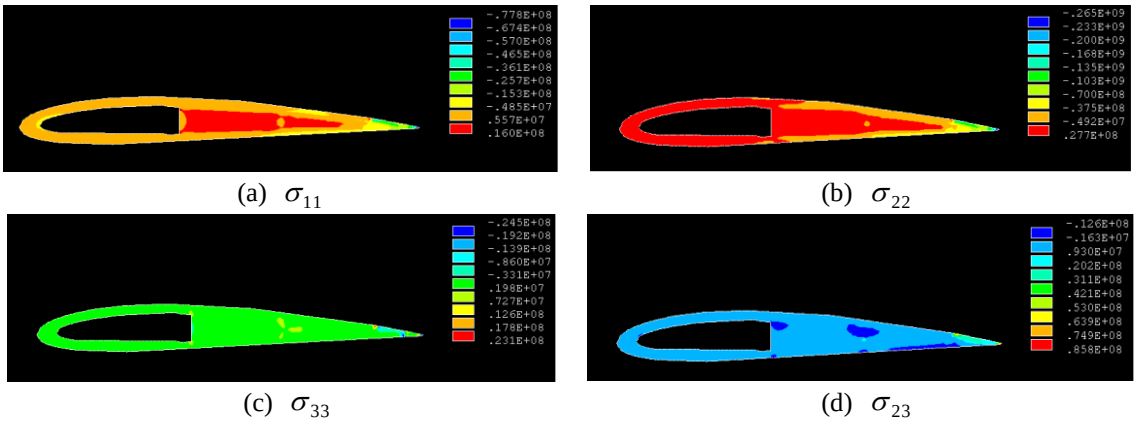

(a) σ_{11} (b) σ_{22}

(c) σ_{33} (d) σ_{23}

Fig. 10 Contour plot of non-zero stress components within the cross-section at mid-span: (a) σ_{11}; (b) σ_{22}; (c) σ_{33}; and (d) σ_{23}

VABS thermal model has the ability of analyzing a realistic blade structure at an affordable computational cost.

A NACA2412 airfoil is used in this case. A schematic of this blade as well as the coordinate

system is depicted in Fig. 9, where x_1 direction is coming out of the page. The chord length l is 0.1524 m while the length of the realistic blade L is 1.524 m. This realistic blade is made of Aluminum as the skin and a typical aerospace foam as the core. The Aluminum has the properties $E = 72.4\text{GPa}$, $\nu = 0.3$, and $\alpha = 22.5\times10^{-6}/^{\circ}\text{C}$, and the properties for the aerospace foam are $E = 2.76$ GPa, $\nu = 0.22$, and $\alpha = 2.2\times10^{-6}/^{\circ}\text{C}$. This blade is cantilevered since most applications like helicopter rotor blade and wind turbine blade can be analyzed as cantilevered beam. A uniform temperature of 100°C is applied to this blade.

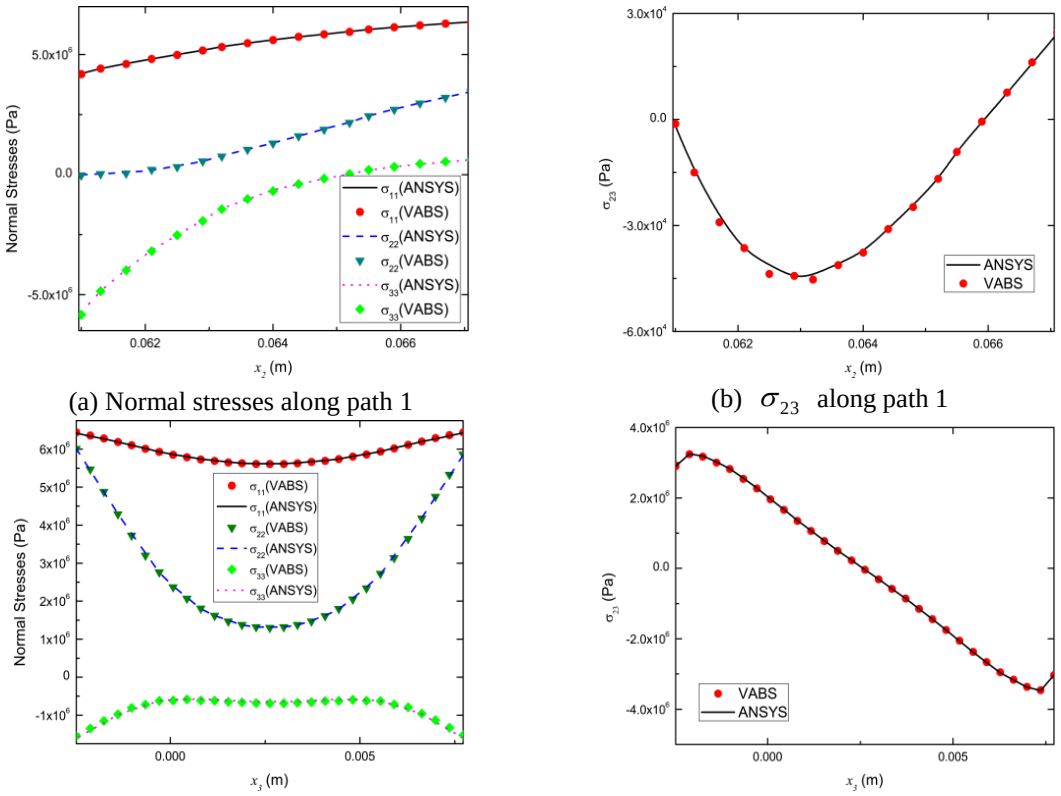

(a) Normal stresses along path 1

(b) σ_{23} along path 1

(c) Normal stresses along path 2

(d) σ_{23} along path 2

Fig. 11 Distributions of non-zero stress components along comparison paths at mid-span: (a) Distributions of normal stresses along comparison path 1; (b) Distribution of σ_{23} along comparison path 1; (c) Distributions of normal stresses along comparison path 2; and (d) Distribution of σ_{23} along comparison path 2

Table 2 Summary of Model Statistics

	ANSYS 3D	VABS
Element Type	SOLID186	8-noded quadrilateral
Number of Elements	362,408	2,459
Number of Nodes	1,638,866	7,965
Running Time	3h 5min 23s	11s + 26s

The contour plots of the non-zero stress components $\sigma_{11}, \sigma_{22}, \sigma_{33}$ and σ_{23} are shown in Fig.10. For quantitative comparison, we plot these non-zero stress components at mid-span of the blade along two comparison paths shown in Fig. 9 in the following figure. From Fig. 11, it is observed that the predictions of VABS have excellent agreement with those of ANSYS 3D along both chord-line-direction (Comparison Path 1) and through-the-thickness (Comparison Path 2) direction.

The computational efficiency of the two models is now shown. Figs.12 and 13 show the mesh used in ANSYS and VABS, respectively. Type of elements used, the total number of elements and nodes in calculations, and the running time of each model are tabulated in Table 2. It needs to be pointed out that the two running times for VABS analysis are for constitutive modeling and recovery, respectively. Both programs are running on a computing server with AMD Opteron(tm) Processor 6174 2.20 GHz (2 processors) and 128 GB RAM. The operating system is 64-bit Windows 7 Professional. It can be observed that the computational cost of VABS calculation is several orders lower than that of 3D analysis.

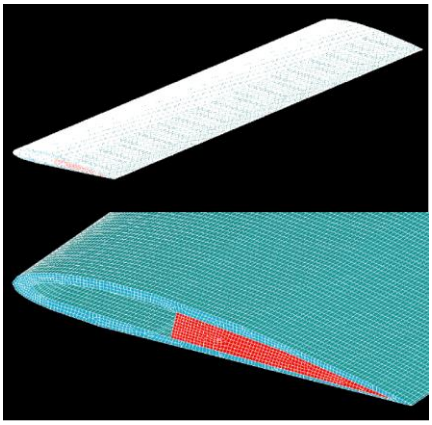

Fig. 12 3D mesh of a realistic blade for Example 3

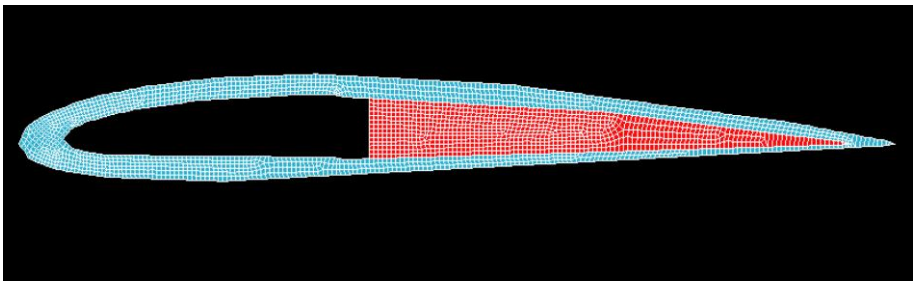

Fig. 13 2D mesh of a realistic blade for VABS calculation

5.4 Example 4: thermoelastic analysis of a composite beam under finite temperature change

In this section, a cantilever two-layer composite beam is used to examine the

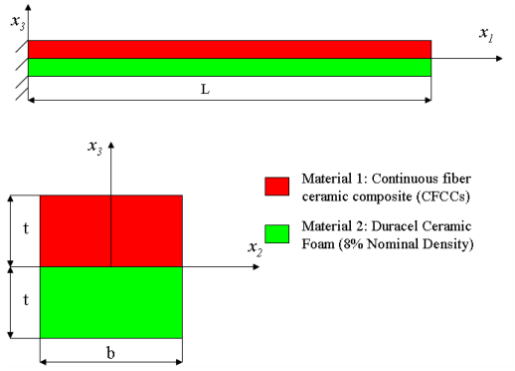

Fig. 14 Schematic of a two-layer composite beam for finite temperature change analysis

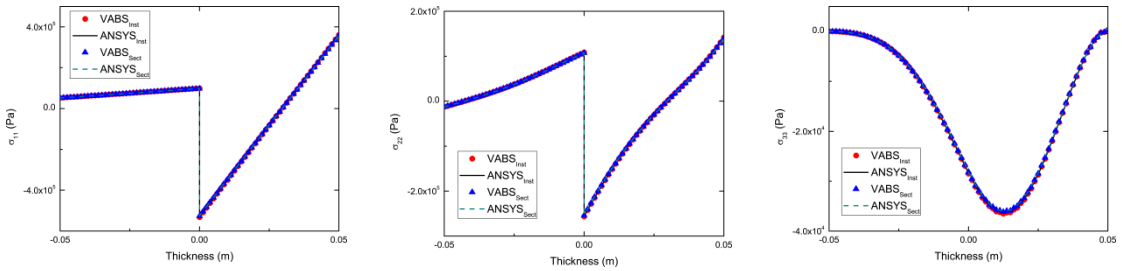

(a) σ_{11} (b) σ_{22} (c) σ_{33}

Fig. 15 Distributions of non-zero stress components along the thickness at $x_2 = 0$ for small temperature change

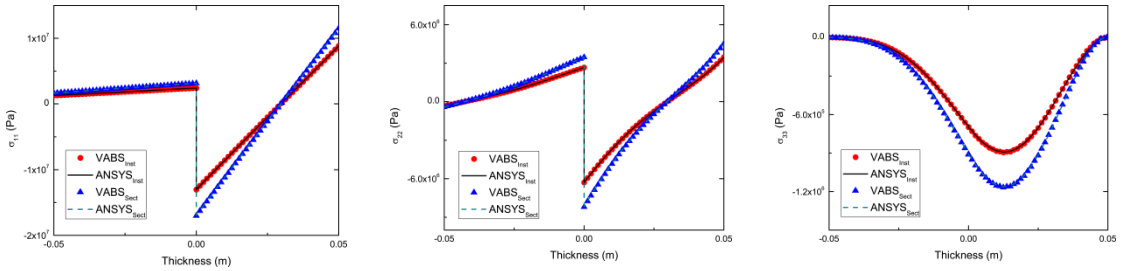

(a) σ_{11} (b) σ_{22} (c) σ_{33}

Fig. 16 Distributions of non-zero stress components along the thickness at $x_2 = 0$ for finite temperature change

Table 3 Material properties of two-layer composite beam in Example 4

	0°C	200°C	500°C
Material 1: CFCCs	$E = 83\text{GPa}$ $\nu = 0.27$ $\alpha = 4.28\times10^{-6}/^{\circ}\text{C}$	$E = 82.47\text{GPa}$ $\nu = 0.27$ $\alpha = 4.278\times10^{-6}/^{\circ}\text{C}$	$E = 81.67\text{GPa}$ $\nu = 0.27$ $\alpha = 4.275\times10^{-6}/^{\circ}\text{C}$
Material 2: DCF	$E = 2.76\text{GPa}$ $\nu = 0.22$ $\alpha = 1.22\times10^{-6}/^{\circ}\text{C}$	$E = 2.76\text{GPa}$ $\nu = 0.22$ $\alpha = 2.06\times10^{-6}/^{\circ}\text{C}$	$E = 2.76\text{GPa}$ $\nu = 0.22$ $\alpha = 2.56\times10^{-6}/^{\circ}\text{C}$

temperature-dependent properties and the framework of thermoelasticity based on finite temperature change. Two load cases are studied here, one is the beam under small temperature change and the other is the beam experiencing finite temperature change. The geometry is given by Fig. 14 with the dimensions $L = 1\text{m}$, $b = 0.1\text{m}$, and $t = 0.05\text{m}$. The material properties are listed in Table 3. Firstly, the beam is experiencing a small temperature change, from 480°C to 500°C. The stress distributions of mid-span along thickness are plotted in Fig. 15. The curves and data points labeled "Inst" are calculated based on the traditional framework of thermoelasticity where instantaneous CTEs are used. The curves and data points labeled "Sect" are from the current framework of thermoelasticity where secant CTEs are used in the analysis. Excellent agreement exists between predictions from VABS and ANSYS 3D analysis. Moreover, due to the small temperature change in this case, the newly developed framework of finite temperature change thermoelasticity does not have a significant impact on the results. In other words, the predictions from traditional constitutive framework of thermoelasticity are adequate for this case.

For the second case, the composite beam is experiencing a large temperature change from 0°C to 500°C. Fig. 16 shows the plots of non-zero stress components σ_{11}, σ_{22}, and σ_{33}, respectively. Again, excellent agreements exist between results from 3D analysis and VABS based on different theories. A striking observation from these three figures is that two different frameworks of thermoelasticity result in huge different stress distributions for this case. It demonstrates that the influence of temperature-dependent material properties and framework of thermoelasticity on thermal stresses is quite significant for finite temperature change cases.

6. Conclusions

The theory for the cross-sectional analysis of beams based on VAM is extended to incorporate thermoelastic analysis. The quasisteady theory of linear thermoelasticity, which neglects the temperature changes due to deformations, is adopted to avoid the fully-coupled thermoelasticity problem. A heat conduction beam model is constructed first to obtained the thermal field. A discussion shows that the current model is also able to handle convection heat transfer problem. Using the solved thermal field as input loads, classic and refined beam models have been developed. The conventional thermoelastic framework is extended for composite materials which removed the restriction on temperature variations and added the dependence of material properties with respect to temperature based on the Kovalenoko's small-strain thermoelasticity theory. All these newly developed beam models are numerically implemented by using finite element method. VABS now is capable of handling thermal problem of composite beams composed of arbitrary materials and geometries. The recovery of 3D field quantities in terms of 1D variables has been derived so that the cross-sectional distributions of displacements, strains, stresses, and thermal field quantities can be obtained.

Acknowledgments

This research is supported, in part, by the Army Vertical Lift Research Center of Excellence at Georgia Institute of Technology and its affiliate program through subcontract at Utah State

University. The technical monitor is Dr. Michael J. Rutkowski.

References

Bapanapalli, S.K., Martinez, O.M., Gogu, C., Sankar, B.V., Haftka, R.T. and Blosser, M.L. (2006), "Analysis and design of corrugated-core sandwich planels for thermal protection systems of space vehicles", *Proceedings of 47th AIAA/ASME/ASCE/AHS/ASC Structures, Structural Dynamics, and Materials Conference*, New Port, USA, May

Berdichevsky, V.L. (1979), "Variational-asymptotic method of constructing a theory of shells", *J. Appl. Math. Mech.*, **43**, 664-687.

Bickford, W.B. (1982), "A consistent higher-order beam theory", *Developments in Theoretical and Applied Mechanics*, **11**, 137-142.

Boley, B.A. and Weiner, J.H. (1997), *Theory of Thermal Stresses*, Dover Publications, Mineola, NY, USA.

Cesnik, C.E.S. and Hodges, D.H. (1993), "Stiffness constants for initially twisted and curved composite beams", *Appl. Mech. Rev.*, **46**, 211-220.

Cook, R.D., Malkus, D.S., Plesha, M.E. and Witt, R.J. (2001), *Concepts and Applications of Finite Element Analysis*, 4th Edition, Wiley, New York, NY, USA.

Copper, C.D. and Pilkey, W.D. (2002), "Thermoelasticity solutions for straight beams", *J. Appl. Mech.*, **69**, 224-229.

Frostig, Y., Baruch, M., Vilnay, O. and Sheinman, I. (1992), "High-order theory for sandwich-beam behavior with transversely flexible core", *J. Eng. Mech.*, **118**, 1026-1043.

Ghiringhelli, G.L. (1997a), "On the linear three-dimensional behavior of composite beams", *Comp. Part B Eng.*, **28**, 613-626.

Ghiringhelli, G.L. (1997b), "On the thermal problem for composite beams using a finite element semi-discretisation", *Comp. Part B Eng.*, **28**, 483-495.

Heyliger, P.R. and Reddy, J.N. (1988), "A higher-order beam finite element for bending and vibration problems", *J. Sound Vib.*, **126**, 309-326.

Hodges, D.H., Atilgan, A.R., Cesnik, C.E.S. and Fulton, M.V. (1992), "On a simplified strain energy function for geometrically nonlinear behavior of anisotropic beams", *Compos. Eng.*, **2**, 513-526.

Huang, D., Ding, H. and Chen, W. (2007), "Analytical solution for functionally graded anisotropic cantilever beam under thermal and uniformly distributed load", *J. Zhejiang Univ. Sci. A*, **8**, 1351-1355.

Kant, T. and Manjunath, B.S. (992), "Refined theories for composite and sandwich beams with C0 finite elements", *Comp. Struct.*, **33**, 755-764.

Kapuria, S., Dumir, P.C. and Ahmed, A. (2003), "An efficient higher order Zigzag theory for composite and sandwich beams subjected to thermal loading", *Int. J. Solids Struct.*, **40**, 6613-6631.

Khdeir, A.A. and Reddy, J.N. (1999), "Jordan canonical form solution for thermally induced deformations of cross-ply laminated composite beams", *Int. J. Solids Struct.*, **22**, 331-346.

Marur, S.R. and Kant, T. (1997), "On the performance of higher order theories for transient dynamic analysis of sandwich and composite beams", *Comp. Struct.*, **65**, 741-759.

Noda, N. (1991), "Thermal stresses in materials with temperature-dependent properties", *Appl. Mech. Rev.*, **44**, 383-397.

Okamoto, N., Kusakari, M., Tanaka, K., Inui, H., Yamaguchi, M. and Otani, S. (2003), "Temperature dependence of thermal expansion and elastic constants of single crystals of ZrB_2 and the suitability of ZrB_2 as a substrate for GaN film", *J. Appl. Phys.*, **93**, 88-93.

Popescu, B. and Hodges, D.H. (2000), "On asymptotically correct Timoshenko-like anisotropic beam theory", *Int. J. Solids Struct.*, **37**, 535-558.

Rao, D.M. and Sinha, P.K. (1997), "Finite element coupled thermostructural analysis of composite beams", *Comp. Struct.*, **63**, 539-549.

Reddy, J.N. (2003), *Mechanics of Laminated Composite Plates and Shells: Theory and Analysis*, (2nd

Edition), CRC Press, Boca Raton, FL, USA.
Reddy, J.N. (2008), *An Introduction to Continuum Mechanics*, Cambridge University Press, New York, NY, USA.
Soldatos, K.P. and Elishakoff, I. (1992), "A transverse shear and normal deformable orthotropic beam theory", *J. Sound Vib.*, **154**, 528-533.
Tanigawa, Y., Murakami, H. and Ootao, Y. (1989), "Transient thermal stress analysis of a laminated composite beam", *J. Therm. Stresses*, **12**, 25-39.
Teng, C., Yu, W. and Chen, M. (2012) "Variational asymptotic homogenization of temperature-dependent heterogeneous materials under finite temperature changes", *Int. J. Solids Struct.*, **49**, 2439-2449.
Vidal, P. and Polit, O. (2006), "A thermomechanical finite element for the analysis of rectangular laminated beams", *Finite Elem. Anal. Des.*, **42**, 868-883.
Wang, Q. and Yu, W. (2011), "Variational asymptotic modeling of the thermal problem of composite beams", *Comp. Struct.*, **93**, 2330-2339.
Wang, Q. and Yu, W. (2013), "A refined model for thermoelastic analysis of initially curved and twisted composite beams", *Eng. Struct.*, **48**, 233-244.
Wikipedia (2011), "Sandwich-structured composite", *Wikipedia, The Free Encyclopedia*, http://en.wikipedia.org/w/index.php?title=Sandwich-structured_composite&oldid=565387616
Yu, W., Hodges, D.H. and Ho, J.C. (2012), "Variational asymptotic beam sectional analysis - an updated version", *Int. J. Eng. Sci.*, **59**, 40-64.
Yu, W., Hodges, D.H., Volovoi, V. and Cesnik, C.E.S. (2002), "On Timoshenko-like modeling of initially curved and twisted composite beams", *Int. J. Solids Struct.*, **39**, 5101-5121.

EC